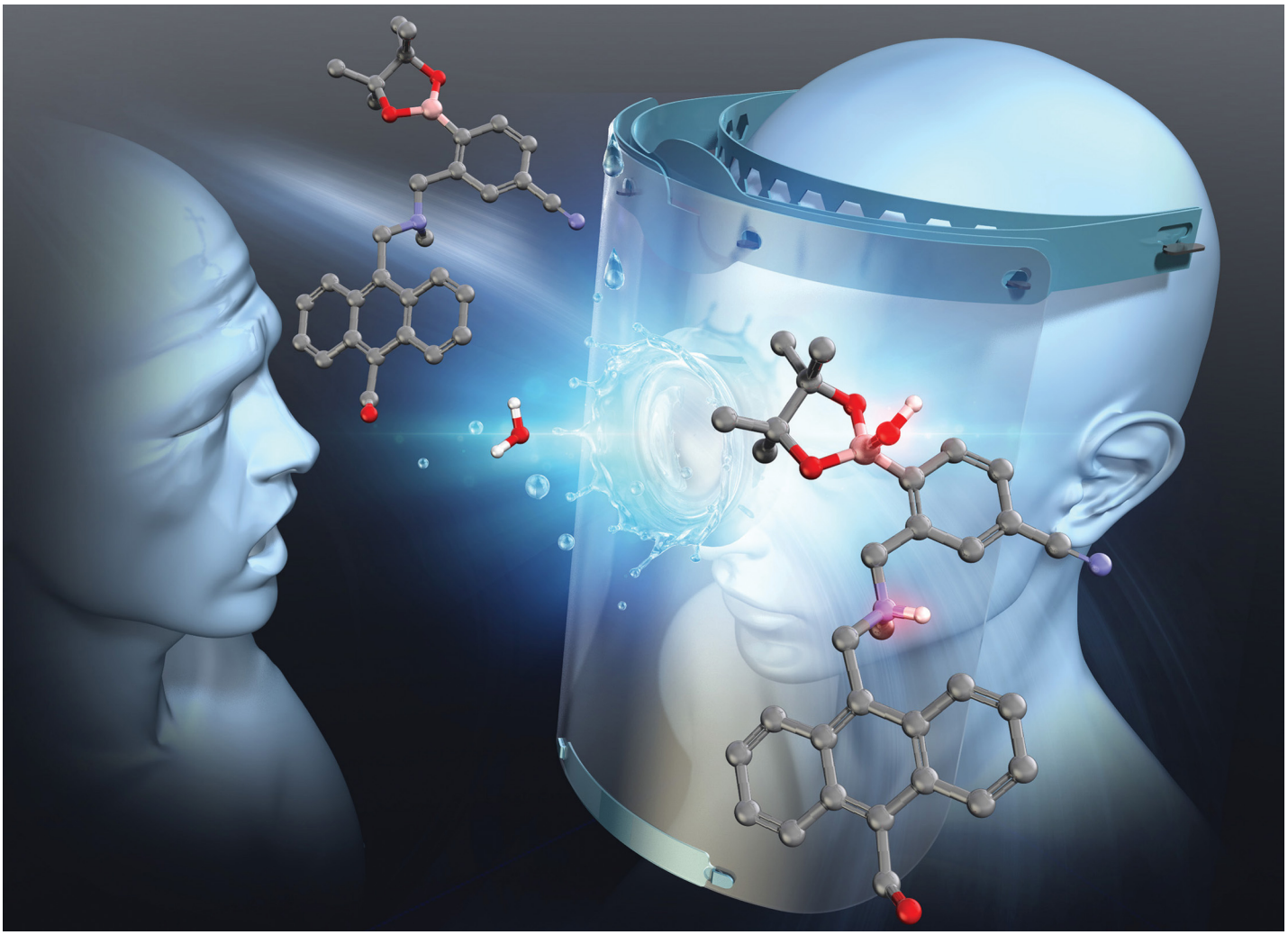

Showcasing research from Professor Yousuke Ooyama's Functional Dye Chemistry laboratory, Department of Applied Chemistry, Graduate School of Engineering, Hiroshima University, Japan.

Development of highly sensitive fluorescent sensor and fluorescent sensor-doped polymer films for trace amounts of water based on photo-induced electron transfer

Anthracene-(aminomethyl)phenylboronic acid pinacol ester having a cyano group as an electron-withdrawing substituent and a hydroxymethyl group has been developed as a highly sensitive PET (photo-induced electron transfer)-type fluorescent sensor for visualization, detection, and quantification of a trace amount of water. Moreover, we demonstrated that the PET-type fluorescent sensor-doped polymer films produce a reversible switching in fluorescent color between the green excimer emission in the PET active state under a drying process and the blue monomer emission in the PET inactive state upon exposure to moisture.

As featured in:

See Yousuke Ooyama *et al.*, *Mater. Adv.*, 2021, **2**, 7662.

ROYAL SOCIETY OF CHEMISTRY

rsc.li/materials-advances

Registered charity number: 207890

Materials Advances

ROYAL SOCIETY OF CHEMISTRY

PAPER

View Article Online
View Journal | View Issue

Cite this: *Mater. Adv.*, 2021, 2, 7662

Development of highly sensitive fluorescent sensor and fluorescent sensor-doped polymer films for trace amounts of water based on photo-induced electron transfer†

Saori Miho,[a] Takuma Fumoto,[a] Yuta Mise,[a] Keiichi Imato,[a] Seiji Akiyama,[b] Mio Ishida[b] and Yousuke Ooyama *[a]

Anthracene-(aminomethyl)phenylboronic acid pinacol ester (AminoMePhenylBPin) **SM-1** having a cyano group as an electron-withdrawing substituent and a hydroxymethyl group has been developed as a highly sensitive PET (photo-induced electron transfer)-type fluorescent sensor for visualization, detection, and quantification of trace amounts of water. **SM-1** shows enhancement of fluorescence with the increase in water content in various solvents (polar, less polar, protic, and aprotic solvents), which is attributed to the suppression of PET due to the formation of the PET inactive (fluorescent) species **SM-1a** by interaction with water molecules. In fact, the formation of **SM-1a** by interaction with water molecules has been successfully detected by ^{1}H NMR spectral measurements. The detection limits (DLs) and quantitation limits (QLs) of **SM-1** for water in solvents are, respectively, 0.006 and 0.018 wt% in 1,4-dioxane, 0.004 and 0.012 wt% in THF, 0.004 and 0.013 wt% in acetonitrile, and 0.007 and 0.021 wt% in ethanol, which are superior to those of **OF-2** without a hydroxymethyl group. This result is attributed to the improvement of fluorescence emission properties by the introduction of a hydroxymethyl group to an anthracene fluorophore. Actually, fluorescence quantum yields (Φ_{fl}) of **OF-2** and **SM-1** in absolute acetonitrile are below 2%, but in acetonitrile with 1 wt% water content the Φ_{fl} of **SM-1** (20%) is higher than that of **OF-2** (13%). Moreover, we have achieved the preparation of various types of polymer films (polystyrene (PS), poly(4-vinylphenol) (PVP), polyvinyl alcohol (PVA), and polyethylene glycol (PEG)) doped with **SM-1**, and investigated the optical sensing properties of the **SM-1**-doped polymer films for water. It was found that the **SM-1**-doped polymer films produce a reversible switching in fluorescence color between the green excimer emission in the PET active state under a drying process and the blue monomer emission in the PET inactive state upon exposure to moisture. Herein, we propose that PET-type fluorescent sensor-doped polymer films based on a fluorescence enhancement system are one of the most promising and convenient functional materials for not only environmental and quality control monitoring systems and industry, but also visualizing the droplet on material surfaces.

Received 24th September 2021,
Accepted 14th October 2021

DOI: 10.1039/d1ma00881a

rsc.li/materials-advances

Introduction

Development of fluorescent sensors for the visualization as well as detection and quantification of trace amounts of water in solutions, solids, and gas or on material surfaces has been of considerable scientific and practical concerns in recent years, with the objective of not only the fundamental study in analytical chemistry, photochemistry, and photophysics, but also their potential applications to environmental and quality control monitoring systems and industry.[1–14] Consequently, fluorescent sensors for water are one of the most promising functional materials contributing to the achievement of the 2030 agenda for Sustainable Development Goals (SDGs), which was adopted by all United Nations Member States in 2015 and provides a shared blueprint for the peace and prosperity of the people and the planet now and in the future. Actually, some kinds of organic fluorescent sensors and polymers for the determination of water content based on ICT (intramolecular charge transfer),[15–24] ESIPT (excited state intramolecular proton transfer),[25–28] PET (photo-induced electron transfer),[29–36] or solvatochromism[37–42] have been designed and synthesized.

[a] *Department of Applied Chemistry, Graduate School of Engineering, Hiroshima University, 1-4-1 Kagamiyama, Higashi-Hiroshima 739-8527, Japan. E-mail: yooyama@hiroshima-u.ac.jp; Fax: +81-82-424-5494*
[b] *Science & Innovation Center, Mitsubishi Chemical Corporation, 1000 Kamoshida-cho, Aoba-ku, Yokohama-Shi, Kanagawa 227-8502, Japan*

† Electronic supplementary information (ESI) available. See DOI: 10.1039/d1ma00881a

The optical sensing properties of these fluorescent sensors for the detection and quantification of water content were investigated from the viewpoints of the relationship between ICT, ESIPT, PET, or solvatochromic characteristics and the intermolecular interaction of the sensors with water molecules. As a result, it was found that most of the previously investigated fluorescent sensors for water, including fluorescent conjugated polymers[43–46] and organic fluorescent dyes with ICT and ESIPT characteristics, are based on a fluorescence quenching (turn-off) system, that is, the fluorescence intensity of the sensors decreases as a function of water content in organic solvents. This fluorescence quenching system makes it difficult to detect trace amounts of water. In contrast, a fluorescence enhancement (turn-on) system exhibiting a fluorescence response with an increase in water content in organic solvents is useful for the visualization, detection, and quantification of trace amounts of water in organic solvents. In particular, the fluorescence enhancement system based on PET-type fluorescent sensors for water can detect a reversible change in its immediate environment due to the reversible intermolecular interactions between the sensors and water molecules. Thus, over the past few decades, we have designed and developed anthracene-(aminomethyl)phenylboronic acid pinacol esters (AminoMePhenylBPin) **OM-1**, **OF-1**, and **OF-2** (Fig. 1a) as PET-type fluorescent sensors for the determination of trace amounts of water. **OF-1** and **OF-2** have a methoxy group as an electron-donating substituent and a cyano group as an electron-withdrawing substituent, respectively, at the *para* position on PhenylBPin.[29–36] In each sensor, the PET takes place from the nitrogen atom of the amino moiety to the photoexcited fluorophore (anthracene) skeleton in the absence of water, leading to fluorescence quenching. The addition of water to organic solvents containing the PET-type fluorescent sensors causes a drastic and linear enhancement of fluorescence emission as a function of water content, which is attributed to the suppression of PET; that is, the nitrogen atom of the amino moiety is protonated or strongly interacts with water molecules, leading to the formation of the PET inactive (fluorescent) species such as **OM-1a**, **OF-1a**, or **OF-2a**.[30,32] Moreover, it was found that the fluorescence sensing ability of the cyano-substituted sensor **OF-2** for water is superior to those of the unsubstituted sensor **OM-1** and the methoxy-substituted sensor **OF-1**. This result can be attributed to the fact that for **OF-2**, the cyano group at the *para* position on PhenylBPin enhances the Lewis acidity of the boron atom due to its electron-withdrawing effect, leading to the facilitation of the formation of the PET inactive (fluorescent) species by interaction with water molecules. In contrast, for **OF-1**, the electron-donating methoxy group at the *para* position on PhenylBPin diminishes the Lewis acidity of the boron atom, leading to the retardation of the formation of the PET inactive (fluorescent) species by the addition of water. Indeed, the detection limits (DLs) and quantitation limits (QLs) of **OF-2** for water were, respectively, 0.01 wt% and 0.03 wt% in 1,4-dioxane, 0.008 wt% and 0.026 wt% in THF, 0.009 wt% and 0.026 wt% in acetonitrile, and 0.009 wt% and 0.027 wt% in ethanol, which are superior to those of **OM-1** and **OF-1**, and are equivalent or superior to those of the fluorescence quenching systems (turn-off) based on the reported ICT-type[15–24] and ESIPT-type[25–28] fluorescent sensors. Thus, the PET method based on the fluorescence enhancement (turn-on) system makes it possible to visualize, detect, and determine trace amounts of water.

Meanwhile, a novel coronavirus, severe acute respiratory syndrome coronavirus 2 (SARS-CoV-2) that causes Coronavirus Disease 2019 (COVID-19), dramatically changed the world to give people a sense of fear of death. Infectious viruses are generally released into the atmosphere through droplet spread from coughing and sneezing by an infected person. Thus, the infection route from an infected person to an uninfected person is predominately due to the droplet. Face shields made of polyester or polycarbonate films and partitions made of acrylic resin are commercially available for reducing the risk of droplet infection. Therefore, if we can visually confirm the droplet on face shields and partitions, this allows us to accurately remove the virus by wiping away the droplet. However, because the virus-containing droplet is generally only 5 μm or more, it is practically difficult for us to visually confirm the droplet. Meanwhile, over 90% of the droplet is composed of water, and thus, techniques and methods capable of visualizing water are undoubtedly useful for detecting the virus-containing droplet. For this purpose, in our previous work, in order to develop fluorescent polymeric materials for visualization and detection of water, we achieved the preparation of various types of polymer films (polystyrene (PS), poly(4-vinylphenol) (PVP), polyvinyl alcohol (PVA), and polyethylene glycol (PEG)) doped with the PET-type fluorescent sensor **OF-2**, and investigated the optical sensing properties of the **OF-2**-doped polymer films for water.[47] It was found that the **OF-2**-doped polymer films exhibit a reversible switching in fluorescence color between the green excimer emission in the PET active state under a drying process and the blue monomer emission in the PET inactive state upon exposure to moisture or water droplets. To the

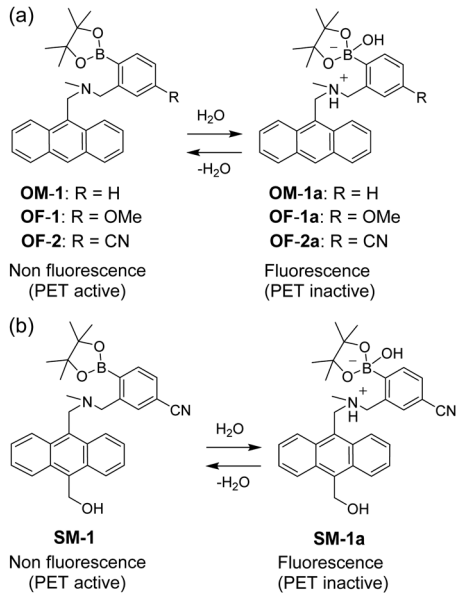

Fig. 1 Mechanisms of PET-type fluorescent sensors (a) **OM-1**, **OF-1**, **OF-2**, and (b) **SM-1** for the detection of water in organic solvents.

best of our knowledge, our previous work was the first to achieve the preparation of PET-type fluorescent sensor-doped polymer films for water, although some fluorescent conjugated polymers[43–46] and ICT-type[22–24] or ESIPT-type[27,28] fluorescent sensor-doped polymer films for water based on a fluorescence quenching (turn-off) system have been prepared. Nevertheless, in order to put the visualization of moisture and water droplets based on the PET method into practical applications, the development of a highly sensitive PET-type fluorescent sensor for trace amounts of water is required.

More recently, in our continuous work to gain insight into the optical sensing mechanism of PET-type fluorescent sensors for water, we found that the DLs and QLs of the PET-type fluorescent sensor **OF-2** are dramatically improved by introducing a hydroxymethyl group on the anthracene skeleton, that is, development of the PET-type fluorescent sensor **SM-1** (Fig. 1b). In this work, the formation of the PET inactive species **OF-2a** and **SM-1a** by interaction with water molecules has been successfully detected by ^{1}H NMR spectral measurements. Furthermore, in order to develop fluorescent polymeric materials for the visualization and detection of water, we have achieved the preparation of various types of polymer films (PS, PVP, PVA, and PEG) doped with **SM-1**, and investigated the optical sensing properties of the **SM-1**-doped polymer films for water. Herein we propose that PET-type fluorescent sensor-doped polymer films based on a fluorescence enhancement system are one of the most promising and convenient functional materials for visualizing virus-containing droplets on the surfaces of face shields and partitions, and as such, will contribute to post-COVID19 society.

Results and discussion

A PET-type fluorescent sensor **SM-1** was prepared by the reaction of (10-((methylamino)methyl)anthracen-9-yl)methanol[48,49] with 3-(bromomethyl)-4-(4,4,5,5-tetramethyl-1,3,2-dioxaborolan-2-yl)benzonitrile (Scheme 1).

In order to investigate the optical sensing ability of **SM-1** for water in 1,4-dioxane and THF as less polar solvents, acetonitrile as a polar solvent, and ethanol as a protic solvent, the photoabsorption and fluorescence spectra of **SM-1** were measured in the solvents containing various concentrations of water (Fig. 2). As with the case of **OF-2**,[32] in all the four solvents, the photoabsorption spectra of **SM-1** show a vibronically structured photoabsorption band in the range of 300 nm to 400 nm originating from the anthracene skeleton and did not undergo

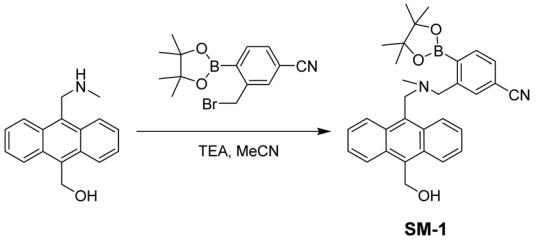

Scheme 1 Synthesis of **SM-1**.

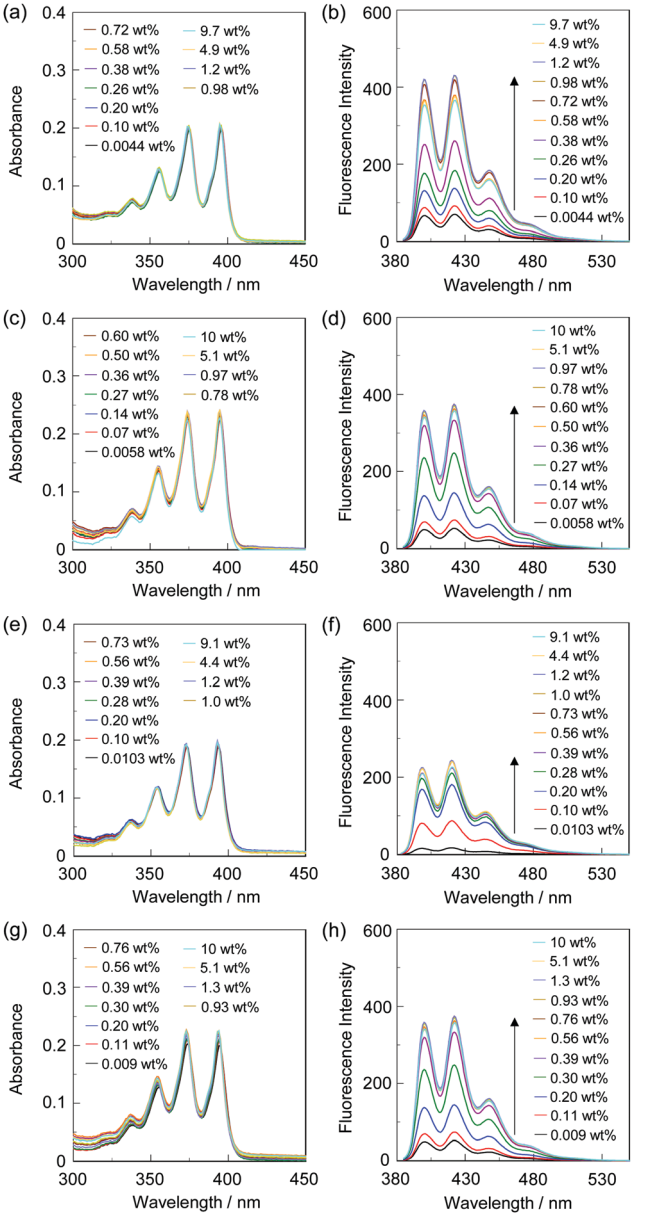

Fig. 2 (a) Photoabsorption and (b) fluorescence spectra (λ^{ex} = 375 nm) of **SM-1** (2.0×10^{-5} M) in 1,4-dioxane containing water (0.0044–9.7 wt%). (c) Photoabsorption and (d) fluorescence spectra (λ^{ex} = 375 nm) of **SM-1** (2.0×10^{-5} M) in THF containing water (0.0058–10 wt%). (e) Photoabsorption and (f) fluorescence spectra (λ^{ex} = 373 nm) of **SM-1** (2.0×10^{-5} M) in acetonitrile containing water (0.0103–9.1 wt%). (g) Photoabsorption and (h) fluorescence spectra (λ^{ex} = 373 nm) of **SM-1** (2.0×10^{-5} M) in ethanol containing water (0.009–10 wt%).

appreciable changes in the absorbance and shape upon the addition of water to the solution (Fig. 2a, c, e and g). In the corresponding fluorescence spectra, **SM-1** in the absolute solvents exhibits a feeble and vibronically structured fluorescence band with a fluorescence maximum wavelength (λ^{fl}_{max}) at around 420 nm in the range of 400 nm to 500 nm in the PET active state, which is attributed to the monomer emission originating from the anthracene skeleton (Fig. 2b, d, f and h). On the other hand, with the increase in the water content in the solutions, the fluorescence

spectra exhibited an enhancement of the monomer emission band with a negligible change in their spectral shapes due to the suppression of PET (the PET inactive state). As shown in Fig. 3a, the acetonitrile solution of **SM-1** did not show visual fluorescence emission, but exhibited blue fluorescence emission upon the addition of water.

In order to estimate the sensitivity and accuracy of **SM-1** for the detection of water in solvent, the changes in the fluorescence peak intensity at around 420 nm were plotted against the water fraction in the solvent (Fig. 4). As with the case of **OF-2** (Fig. S2, ESI†),[32] the plots of **SM-1** demonstrated that the fluorescence peak intensity increased linearly as a function of the water content in all four solvents (Fig. 4a). Thus, the DLs and QLs of **SM-1** for water in the solvents were determined based on the following equations: DL = $3.3\sigma/m_s$ and QL = $10\sigma/m_s$, where σ is the standard deviation of the blank sample and m_s is the slope of a calibration curve obtained from the plot of the fluorescence peak intensity at around 420 nm *versus* the water fraction in the low water content region below 1.0 wt% (Fig. 4b). The results are as follows:

$$\text{1,4-Dioxane: } F = 564.2[H_2O] + 43.8\ (R^2 = 0.983,\ [H_2O] = 0.0044\text{–}0.58\ \text{wt\%}) \quad (1)$$

$$\text{THF: } F = 819.6[H_2O] + 31.5\ (R^2 = 0.989,\ [H_2O] = 0.0058\text{–}0.36\ \text{wt\%}) \quad (2)$$

$$\text{Acetonitrile: } F = 753.5[H_2O] + 13.1\ (R^2 = 0.975,\ [H_2O] = 0.0103\text{–}0.28\ \text{wt\%}) \quad (3)$$

$$\text{Ethanol: } F = 484.2[H_2O] + 12.6\ (R^2 = 0.979,\ [H_2O] = 0.009\text{–}0.30\ \text{wt\%}) \quad (4)$$

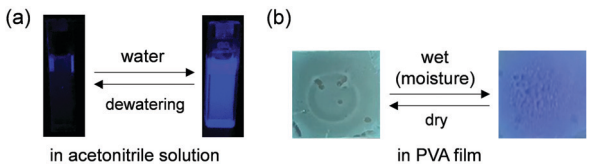

Fig. 3 Photographs (under 254 nm irradiation) of (a) acetonitrile solution of **SM-1** before and after addition of water and (b) 50 wt% **SM-1**-doped PVA film before and after exposure to moisture.

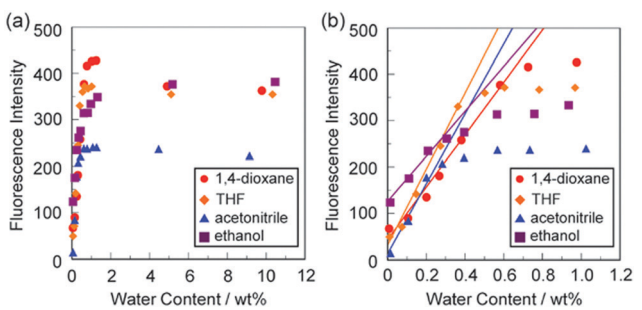

Fig. 4 Fluorescence peak intensity at around 420 nm of **SM-1** (λ^{ex} = 373–375 nm) as a function of water content below (a) 10 wt% and (b) 1.0 wt% in 1,4-dioxane, THF, acetonitrile, and ethanol.

Indeed, the correlation coefficient (R^2) values for the calibration curves of **SM-1** are 0.975–0.989, which indicates good linearity, as with the case of **OF-2**. However, a large difference in the m_s values between **SM-1** and **OF-2** was observed; that is, the m_s values for **SM-1** are, respectively, 564 in 1,4-dioxane, 819 in THF, 753 in acetonitrile, and 484 in ethanol and much larger than those of **OF-2** (Table 1). The large m_s values for **SM-1** relative to **OF-2** can be attributed to the improvement in the fluorescence emission property by the introduction of a hydroxymethyl group to an anthracene fluorophore. Actually, fluorescence quantum yields (Φ_{fl}) of **OF-2** and **SM-1** in absolute acetonitrile are below 2%, but in acetonitrile with 1 wt% water content the Φ_{fl} (20%) of **SM-1** is higher than that (13%) of **OF-2**. The DLs and QLs of **SM-1** for water are, respectively, 0.006 and 0.018 wt% in 1,4-dioxane, 0.004 and 0.012 wt% in THF, 0.004 and 0.013 wt% in acetonitrile, and 0.007 and 0.021 wt% in ethanol, which are superior to those of **OF-2**. Consequently, it was found that the anthracene-AminoMePhenylBPin-based sensor **SM-1**, with a cyano group as an electron-withdrawing substituent and a hydroxymethyl group, is a highly sensitive PET-type fluorescent sensor for the detection and quantification of trace amounts of water in polar, less polar, protic, and aprotic solvents.

In order to confirm the mechanism of the PET-type fluorescent sensor based on the anthracene-AminoMePhenylBPin structure for the detection of water, we performed ^{1}H NMR spectral measurements of **OF-2** and **SM-1** with and without the addition of water in the acetonitrile-d_3 solution (2.0×10^{-2} M) (Fig. 5 and 6). Both the ^{1}H NMR spectra of **OF-2** and **SM-1** solution (containing water content of 0.46 wt% and 0.18 wt%, respectively) without the addition of water show obvious signals which can be assigned to a single chemical species with **OF-2** and **SM-1** structures. On the other hand, for both the ^{1}H NMR spectra of **OF-2** and **SM-1** solution with water content of 2.6 wt% and 2.8 wt%, respectively, some additional signals appear at both the aliphatic and aromatic regions, compared to that of the solution without the addition of water. Indeed, the ^{1}H NMR spectra in the solutions with a water content of

Table 1 DL and QL of **OF-2**, **SM-1**, and previously reported ICT-type and ESIPT-type fluorescent sensors for water in various organic solvents

Sensor	Solvent	m_s[a]	DL[b]	QL[b]
OF-2[32]	1,4-Dioxane	334	0.01 wt%	0.03 wt%
	THF	390	0.008 wt%	0.026 wt%
	Acetonitrile	382	0.009 wt%	0.026 wt%
	Ethanol	362	0.009 wt%	0.027 wt%
SM-1	1,4-Dioxane	564	0.006 wt%	0.018 wt%
	THF	819	0.004 wt%	0.012 wt%
	Acetonitrile	753	0.004 wt%	0.013 wt%
	Ethanol	484	0.007 wt%	0.021 wt%
ICT-type[15]	1,4-Dioxane	−40.23	0.008 wt%	No data
	Acetonitrile	−52.10	0.006 wt%	No data
	Ethanol	−22.42	0.015 wt%	No data
ESIPT-type[26]	1,4-Dioxane	−5.46	0.053 wt%	No data
	THF	−10.38	0.006 wt%	No data
	Acetonitrile	−7.63	0.011 wt%	No data

[a] Slope of calibration curve. [b] Detection limit (DL) and quantitation limit (QL) of the sensor for water.

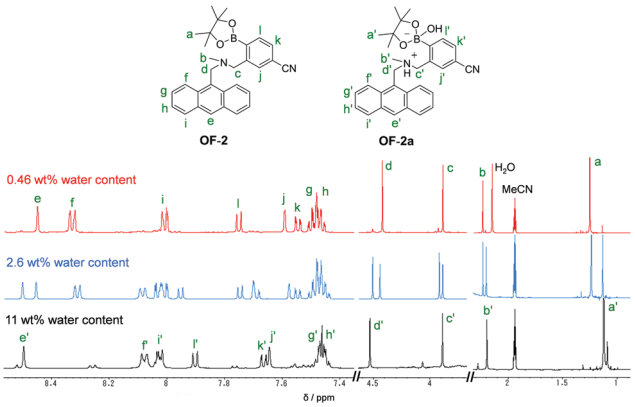

Fig. 5 ^{1}H NMR spectra of **OF-2** (2.0×10^{-2} M) in acetonitrile-d_3 with 0.46 wt%, 2.6 wt% and 11 wt% water content.

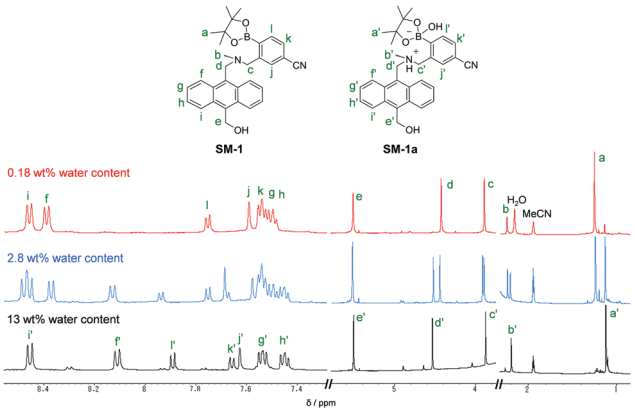

Fig. 6 ^{1}H NMR spectra of **SM-1** (2.0×10^{-2} M) in acetonitrile-d_3 with 0.18 wt%, 2.8 wt% and 13 wt% water content.

2.6–2.8 wt% clearly indicate the existence of another chemical species as well as **OF-2** and **SM-1**. Moreover, both the ^{1}H NMR spectra of **OF-2** and **SM-1** solution with a water content of 11 wt% and 13 wt%, respectively can be assigned to a single chemical species which is quite different from the **OF-2** and **SM-1** structure, that is, the PET inactive species **OF-2a** and **SM-1a** (Fig. 1) occur upon the addition of water to the **OF-2** and **SM-1** solution, respectively. Consequently, upon the addition of water to **OF-2** and **SM-1** solution, the chemical shifts of the methyl protons H_a of boronic acid pinacol ester and the aromatic protons H_e and H_f of the anthracene skeleton show a considerable upfield shift, but the chemical shifts of H_j, H_k and H_l of the phenyl group and the methylene protons H_d on the anthracene skeleton show a considerable downfield shift. Furthermore, for the ^{1}H NMR spectrum of the **SM-1** solution with the addition of water, it is worth noting here that there is no appreciable change in chemical shifts for the methylene protons H_e of the hydroxymethyl group on an anthracene skeleton (Fig. 6). This fact indicates that for **SM-1** the hydroxymethyl group does not act as a proton donor or acceptor which may affect the formation of the PET inactive species **SM-1a** through interaction with water molecules.

Next, in order to investigate the optical properties of **SM-1** in the aggregate state, the spin-coated **SM-1** film was prepared on a glass substrate, and the photoabsorption and fluorescence spectra of the spin-coated **SM-1** film before and after exposure to moisture were repeatedly measured several times (Fig. 7). As with the case of **OF-2** (Fig. S3, ESI†),[47] the as-prepared spin-coated **SM-1** film (in the dry process) shows a vibronically-structured photoabsorption band in the range of 300 nm to 400 nm originating from the anthracene skeleton (Fig. 7a). The photoabsorption spectral shape of the spin-coated **SM-1** film did not undergo appreciable changes upon exposure to moisture, although a slight change in the absorbance during the repeated cycles was observed due to the disturbance of the baseline in the photoabsorption spectra. In the corresponding fluorescence spectra, the as-prepared spin-coated **SM-1** film shows a broad fluorescence band in the range of 400 nm to 600 nm, which is assigned to the excimer emission originating from the anthracene skeleton in the PET active state (Fig. 7b). Interestingly, the spin-coated **SM-1** film underwent a change in the fluorescence spectra upon exposure to moisture (in the wet process), which caused the vibronically-structured monomer emission (λ^{fl}_{max} = *ca.* 420 nm) in the range of 400 nm to 500 nm arising from the PET inactive state. Moreover, it was found that when the spin-coated **SM-1** film after exposure to moisture was dried in the atmosphere, the photoabsorption and fluorescence spectra showed the original spectral shapes before exposure to moisture, as with the case of **OF-2**. However, there is a difference in the ratio (Fl_{mon}/Fl_{exm}) of the intensity of the monomer to excimer emission between the spin-coated **SM-1** and **OF-2** film. The Fl_{mon}/Fl_{exm} of the spin-coated **OF-2** film is higher than that of the spin-coated **SM-1** film, that is, for the spin-coated **OF-2** film, the Fl_{mon} is much larger than Fl_{exm}, but for the spin-coated **SM-1** film, the Fl_{mon} is almost equal to Fl_{exm}. This result might be attributed to the idea that for **SM-1** in the aggregate state, the excimer formation is facilitated by intermolecular hydrogen bonding between the hydroxymethyl groups. Thus, for the spin-coated **SM-1** film, the reversibility of the fluorescence intensity between the excimer and monomer emissions in the dry-wet process was investigated

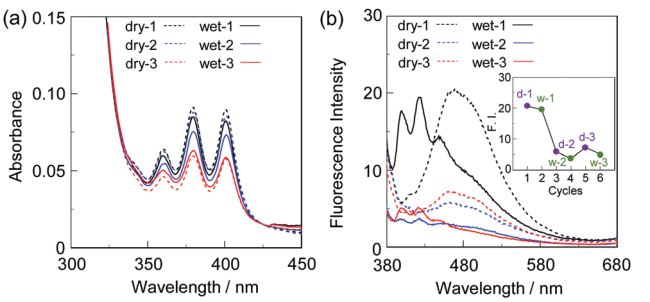

Fig. 7 (a) Photoabsorption and (b) fluorescence spectra (λ^{ex} = 360 nm) of the spin-coated **SM-1** film before (in dry process) and after (in wet process) exposure to moisture. For the photoabsorption spectra, baseline-correction has been made to be the same absorbance at 425 nm for all the spectra. The inset in (b) shows reversible switching of fluorescence intensity at around 480 nm in the dry process and at 420 nm in the wet process of the spin-coated **SM-1** film.

(Fig. 7b inset). The dry-wet cycle shows that the monomer emission disappeared almost completely in the second wet process, as with the case of **OF-2** (Fig. S3b inset, ESI†).[47] The poor reversibility of the fluorescence intensity of the spin-coated **SM-1** and **OF-2** films between the excimer and monomer emissions may be attributed to destruction of the film during the dry-wet process.

In order to investigate the possibility for **SM-1** to function in polymeric materials for the visualization and detection of water, we prepared various types of polymer films (PS, PVP, PVA, and PEG) doped with **SM-1** at 50 wt%, and the photoabsorption and fluorescence spectra of the **SM-1**-doped polymer films before and after exposure to moisture were repeatedly measured several times (Fig. 8). As with the case of **OF-2** (Fig. S4, ESI†),[47] the as-prepared **SM-1**-doped polymer films (in the dry process) show a vibronically structured photoabsorption band in the range of 300 nm to 400 nm and a broad fluorescence band in the range of 400 nm to 600 nm attributable to the excimer emission originating from the anthracene skeleton in the PET active state (Fig. 8). When the **OF-2**-doped polymer films were exposed to moisture (in the wet process), the photoabsorption spectral shape did not undergo appreciable changes, although a slight change in the absorbance was observed due to the disturbance of the baseline in the photoabsorption spectra. The corresponding fluorescence spectra show a change in spectral shape from the broad excimer emission to the vibronically structured monomer emission (λ^{fl}_{max} = 415 nm) arising from the PET inactive state upon exposure to moisture. In fact, one can see that an as-prepared **SM-1**-doped PVA film initially exhibits the green excimer emission in the PET active state, but the blue monomer emission in the PET inactive state upon exposure to moisture or water droplets (Fig. 3b). It is worth mentioning here that there are differences in the Fl_{mon}/Fl_{exm} of the intensity of the monomer to excimer emission between the four types of polymer films. For the **SM-1**-doped PS and PVP films, the Fl_{exm} is larger than Fl_{mon}, but for the **SM-1**-doped PVA and PEG films, the Fl_{mon} is larger than Fl_{exm}. In contrast, for all four **OF-2**-doped polymer films, the Fl_{mon} is larger than Fl_{exm}. This result suggests that for **SM-1** in the polymer films, the excimer formation is facilitated in the hydrophobic PS and PVP films suitable for the formation of intermolecular hydrogen bonding between the hydroxymethyl groups, rather than in the hydrophilic PVA and PEG films. Indeed, for the fluorescence spectra of the **SM-1**-doped PS and PVP films, it is practically difficult to distinguish between the monomer and excimer emissions before and after exposure to moisture. The dry-wet cycles of the **SM-1**-doped polymer films show that for the **SM-1**-doped PVA and PEG films, a reversible switching in fluorescence intensity between the excimer and monomer emissions was obviously still observed in the third dry-wet process (Fig. 9). This result might be attributed to the idea that **SM-1** has good compatibility with the hydrophilic PVA and PEG films rather than the hydrophobic PS and PVP films. In addition, the reversibility of the fluorescence intensity of the **SM-1**-doped PVA and PEG films is superior to that of the spin-coated **SM-1** film (Fig. 7b inset). Therefore, it was found that for **SM-1**, the hydrophilic PVA and PEG films produce a good

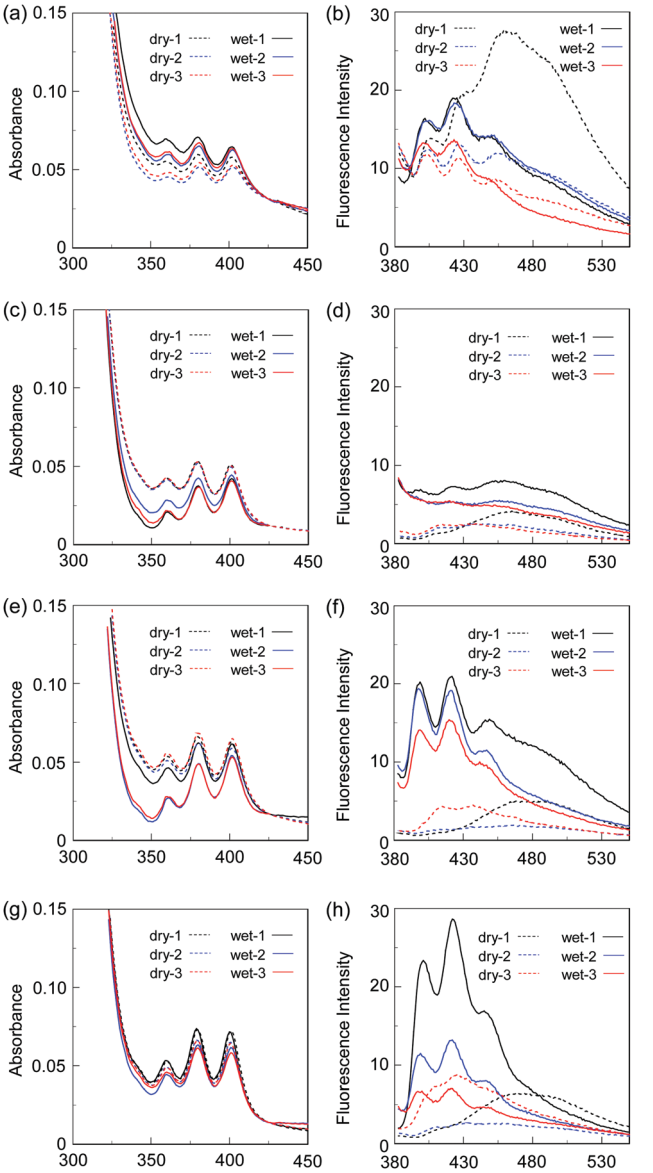

Fig. 8 (a) Photoabsorption and (b) fluorescence spectra (λ^{ex} = 360 nm) of the spin-coated PS film with 50 wt% **SM-1** before (in dry process) and after (in wet process) exposure to moisture. (c) Photoabsorption and (d) fluorescence spectra (λ^{ex} = 360 nm) of the spin-coated PVP film with 50 wt% **SM-1** before (in dry process) and after (in wet process) exposure to moisture. (e) Photoabsorption and (f) fluorescence spectra (λ^{ex} = 360 nm) of the spin-coated PVA film with 50 wt% **SM-1** before (in dry process) and after (in wet process) exposure to moisture. (g) Photoabsorption and (h) fluorescence spectra (λ^{ex} = 360 nm) of the spin-coated PEG film with 50 wt% **SM-1** before (in dry process) and after (in wet process) exposure to moisture. For all the photoabsorption spectra, baseline-correction has been made to be the same absorbance at 425 nm.

reversibility and a large change in the intensity between the excimer and monomer emissions during the dry-wet process, compared to the hydrophobic PS and PVP films, although all four **OF-2**-doped polymer films have a relatively good reversibility of the fluorescence intensity for moisture (Fig. S5, ESI†).[47] Consequently, this work demonstrated that highly sensitive PET-type fluorescent sensor-doped polymer films exhibit a

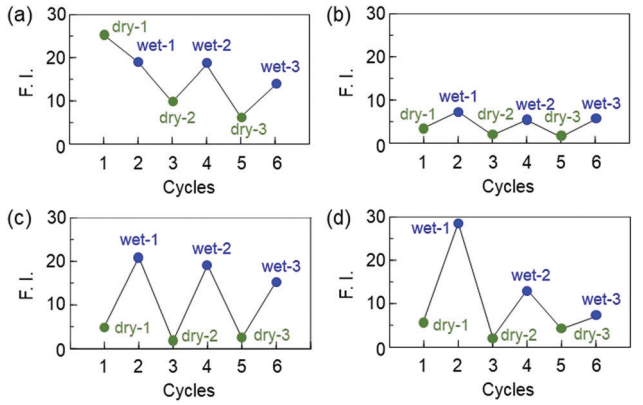

Fig. 9 Reversible switching of fluorescence intensity at around 480 nm in the dry process and at 420 nm in the wet process of 50 wt% **SM-1**-doped (a) PS, (b) PVP, (c) PVA, and (d) PEG films.

reversible switching between the excimer and monomer emissions during the dry-wet process, that is, enable the visualization and detection of moisture and water droplets.

Conclusions

We have developed a highly sensitive PET-type fluorescent sensor based on the anthracene-AminoMePhenylBPin structure, **SM-1** having a cyano group as an electron-withdrawing substituent and a hydroxymethyl group, for visualization, detection, and quantification of trace amounts of water. In fact, the formation of the PET inactive species **SM-1a** by interaction with water molecules has been successfully detected by ^{1}H NMR spectral measurements. It was found that the introduction of a cyano group and a hydroxymethyl group to an anthracene-AminoMePhenylBPin structure can improve the sensitivity and accuracy of the PET-type fluorescent sensor for water. Moreover, we have achieved the preparation of various types of polymer films (PS, PVP, PVA, and PEG) doped with **SM-1**, and demonstrated that the **SM-1**-doped polymer films produce a reversible switching in fluorescence color between the green excimer emission in the PET active state under a drying process and the blue monomer emission in the PET inactive state upon exposure to moisture. Consequently, this work proposes that highly sensitive PET-type fluorescent sensor-doped polymer films are one of the most promising and convenient fluorescent polymeric materials for visualization and detection of moisture and water droplets.

Experimental

General

Melting points were measured using AS ONE ATM-02. IR spectra were recorded using a SHIMADZU IRTracer-100 spectrometer by the ATR method. ^{1}H and ^{13}C NMR spectra were recorded using a Varian-400 or Varian-500 FT NMR spectrometer. High-resolution mass spectral data obtained by APCI were acquired using Thermo Fisher Scientific LTQ Orbitrap XL. Photoabsorption spectra were observed using a SHIMADZU UV-3600 plus or UV-3150 spectrophotometer. Fluorescence spectra were measured using a Hitachi F-4500 spectrophotometer. The fluorescence quantum yields were determined using a Hamamatsu C9920-01 equipped with CCD using a calibrated integrating sphere system. The addition of water to 1,4-dioxane, THF, acetonitrile, or ethanol solutions containing **SM-1** was made in terms of weight percent (wt%). The determination of water in solvents was performed using an MKC-610 and MKA-610 Karl Fischer moisture titrator (Kyoto Electronics Manufacturing Co., Ltd) based on Karl Fischer coulometric titration for below 1.0 wt% and volumetric titration for 1.0–10 wt%.

Synthesis

3-((((10-(Hydroxymethyl)anthracen-9-yl)methyl)(methyl)amino)methyl)-4-(4,4,5,5-tetramethyl-1,3,2-dioxaborolan-2-yl)benzonitrile (SM-1). A solution of (10-((methylamino)methyl)anthracen-9-yl)methanol[48,49] (0.25 g, 1.00 mmol), 3-(bromomethyl)-4-(4,4,5,5-tetramethyl-1,3,2-dioxaborolan-2-yl)benzonitrile (0.32 g, 1.00 mmol), triethylamine (0.55 mL, 3.96 mmol), and acetonitrile (33 mL) was stirred for 4 h at 80 °C under a nitrogen atmosphere. After concentrating under reduced pressure, the resulting residue was chromatographed on alumina (methanol : dichloromethane = 1 : 40 as eluent) to give **SM-1** (0.35 g, yield 71%) as a light yellow solid; m.p. 95–99 °C; FT-IR (ATR): $\tilde{\nu}$ = 2978, 2228, 1447, 1344, 1271, 1142 cm^{-1}; ^{1}H NMR (400 MHz, acetone-d_6): δ = 1.29 (s, 12H), 2.29 (s, 3H), 4.01 (s, 2H), 4.48 (s, 2H), 5.60 (d, J = 5.4Hz, 2H), 7.49–7.56 (m, 4H), 7.64 (dd, J = 1.6 and 7.6 Hz, 1H), 7.74 (s, 1H), 7.88 (d, J = 7.6 Hz, 1H), 8.45 (dd, J = 3.3 and 7.7 Hz, 2H), 8.53 (dd, J = 3.5 and 7.9 Hz, 2H) ppm; ^{13}C NMR (125 MHz, $CDCl_3$): δ = 25.14, 42.95, 52.33, 57.52, 60.70, 83.95, 113.35, 119.21, 124.54, 125.50, 125.74, 125.93, 129.68, 129.94, 130.98, 131.34, 131.78, 131.87, 135.36, 146.18 ppm; HRMS (APCI): m/z (%): [M$^{+\bullet}$] calcd for $C_{31}H_{33}N_2O_3B$, 492.25787; found 492.25879.

Preparation of SM-1-doped polymer films

Polystyrene (PS), poly(4-vinylphenol) (PVP), or polyethylene glycol (PEG) (5 mg) was dissolved in a THF solution (1 mL) of **SM-1** (5 mg) to form a 50 wt% stock solution. On the other hand, a THF solution (0.5 mL) of **SM-1** (5 mg) was added to a polyvinyl alcohol (PVA) (5 mg) aqueous solution (0.5 mL) around 50 °C to form a 50 wt% stock solution. To prepare a polymer film, 300 μL of an **SM-1**-polymer solution was directly spin-coated (3000 rpm for 30 s) on a glass substrate (MIKASA MS-A-100 Opticoat Spincoater). The spin-coated films were dried in air. The resulting **SM-1**-doped polymer films were exposed to moisture for 60 s using a humidifier.

Conflicts of interest

There are no conflicts to declare.

Acknowledgements

This work was supported by Grants-in-Aid for Scientific Research (B) from the Japan Society for the Promotion of

Science (JSPS) KAKENHI Grant Number 19H02754 and JST Adaptable and Seamless Technology transfer Program through Target-driven R&D (A-STEP) Grant Number JPMJTM20RB.

Notes and references

1 H. S. Jung, P. Verwilst, W. Y. Kim and J. S. Kim, Fluorescent and colorimetric sensors for the detection of humidity or water content, *Chem. Soc. Rev.*, 2016, **45**, 1242–1256.
2 P. Kumar, R. Sakla, A. Ghosh and D. A. Jose, Reversible Colorimetric Sensor for Moisture Detection in Organic Solvents and Application in Inkless Writing, *ACS Appl. Mater. Interfaces*, 2017, **9**, 25600–25605.
3 Y. Zhou, G. Baryshnikov, X. Li, M. Zhu, H. Ågren and L. Zhu, Anti-Kasha's Rule Emissive Switching Induced by Intermolecular H-Bonding, *Chem. Mater.*, 2018, **30**, 8008–8016.
4 F. Wu, L. Wang, H. Tang and D. Cao, Excited State Intramolecular Proton Transfer Plus Aggregation-Induced Emission-Based Diketopyrrolopyrrole Luminogen: Photophysical Properties and Simultaneously Discriminative Detection of Trace Water in Three Organic Solvents, *Anal. Chem.*, 2019, **91**, 5261–5269.
5 S. Mishra and A. K. Singh, Optical sensors for water and humidity and their further applications, *Coord. Chem. Rev.*, 2021, **445**, 214063.
6 S. Song, Y. Zhang, Y. Yang, C. Wang, Y. Zhou, C. Zhang, Y. Zhao, M. Yang and Q. Lin, Ratiometric fluorescence detection of trace water in organic solvents based on aggregation-induced emission enhanced Cu nanoclusters, *Analyst*, 2018, **143**, 3068–3074.
7 H. Yan, S. Guo, F. Wu, P. Yu, H. Liu, Y. Li and L. Mao, Carbon Atom Hybridization Matters: Ultrafast Humidity Response of Graphdiyne Oxides, *Angew. Chem., Int. Ed.*, 2018, **57**, 3922–3926.
8 T. Maeda and F. Würthner, Halochromic and hydrochromic squaric acid functionalized perylene bisimide, *Chem. Commun.*, 2015, **51**, 7661–7664.
9 W. Cheng, Y. Xie, Z. Yang, Y. Sun, M.-Z. Zhang, Y. Ding and W. Zhang, General Strategy for in Situ Generation of a Coumarin-Cu^{2+} Complex for Fluorescent Water Sensing, *Anal. Chem.*, 2019, **91**, 5817–5823.
10 J. Othong, J. Boonmak, F. Kielar and S. Youngme, Dual Function Based on Switchable Colorimetric Luminescence for Water and Temperature Sensing in Two-Dimensional Metal–Organic Framework Nanosheets, *ACS Appl. Mater. Interfaces*, 2020, **12**, 41776–41784.
11 S. Roy, S. Das, A. Ray and P. P. Parui, An inquisitive fluorescence method for the real-time detection of trace moisture in polar aprotic solvents with the application of water rancidity in foodstuffs, *New J. Chem.*, 2021, **45**, 4574–4583.
12 K. Nishino, H. Yamamoto, J. Ochi, K. Tanaka and Y. Chujo, Time-Dependent Emission Enhancement of the Ethynylpyrene-o-Carborane Dyad and Its Application as a Luminescent Color Sensor for Evaluating Water Contents in Organic Solvents, *Chem. – Asian J.*, 2019, **14**, 1577–1581.
13 K. Tanaka, K. Nishino, S. Ito, H. Yamane, K. Suenaga, K. Hashimoto and Y. Chujo, Development of solid-state emissive o-carboranes and theoretical investigation of the mechanism of the aggregation-induced emission behaviors of organoboron ''element-blocks'', *Faraday Discuss.*, 2017, **196**, 31–42.
14 H. Mori, K. Nishino, K. Wada, Y. Morisaki, K. Tanaka and Y. Chujo, Modulation of luminescence chromic behaviors and environment-responsive intensity changes by substituents in bis-*o*-carborane-substituted conjugated molecules, *Mater. Chem. Front.*, 2018, **2**, 573–579.
15 C.-G. Niu, P.-Z. Qin, G.-M. Zeng, X.-Q. Gui and A.-L. Guan, Fluorescence sensor for water in organic solvents prepared from covalent immobilization of 4-morpholinyl-1, 8-naphthalimide, *Anal. Bioanal. Chem.*, 2007, **387**, 1067–1074.
16 Z. Li, Q. Yang, R. Chang, G. Ma, M. Chen and W. Zhang, *N*-Heteroaryl-1,8-naphthalimide fluorescent sensor for water: Molecular design, synthesis and properties, *Dyes Pigm.*, 2011, **88**, 307–314.
17 W. Chen, Z. Zhang, X. Li, H. Ågren and J. Su, Highly sensitive detection of low-level water content in organic solvents and cyanide in aqueous media using novel solvatochromic AIEE fluorophores, *RSC Adv.*, 2015, **5**, 12191–12201.
18 S. Tsumura, T. Enoki and Y. Ooyama, A colorimetric and fluorescent sensor for water in acetonitrile based on intramolecular charge transfer: D–$(\pi$–A$)_2$-type pyridine–boron trifluoride complex, *Chem. Commun.*, 2018, **54**, 10144–10147.
19 T. Enoki and Y. Ooyama, Colorimetric and ratiometric fluorescence sensing of water based on 9-methyl pyrido[3,4-*b*]indole-boron trifluoride complex, *Dalton Trans.*, 2019, **48**, 2086–2092.
20 K. Imato, T. Enoki and Y. Ooyama, Development of an intramolecular charge transfer-type colorimetric and fluorescence sensor for water by fusion with a juloidine structure and complexation with boron trifluoride, *RSC Adv.*, 2019, **9**, 31466–31473.
21 S. Tusmura, K. Ohira, K. Imato and Y. Ooyama, Development of optical sensor for water in acetonitrile based on propeller-structured BODIPY-type pyridine–boron trifluoride complex, *RSC Adv.*, 2020, **10**, 33836–33843.
22 D. Citterio, K. Minamihashi, Y. Kuniyoshi, H. Hisamoto, S. Sasaki and K. Suzuki, Optical determination of low-level water concentrations in organic solvents using fluorescent acridinyl dyes and dye-immobilized polymer membranes, *Anal. Chem.*, 2001, **73**, 5339–5345.
23 C.-G. Niu, A.-L. Guan, G.-M. Zeng, Y.-G. Liu and Z.-W. Li, Fluorescence water sensor based on covalent immobilization of chalcone derivative, *Anal. Chim. Acta*, 2006, **577**, 264–270.
24 Z.-Z. Li, C.-G. Niu, G.-M. Zeng and P.-Z. Qin, Fluorescence Sensor for Water Content in Organic Solvents Based on Covalent Immobilization of Benzothioxanthene, *Chem. Lett.*, 2009, **38**, 698–699.
25 W. Liu, Y. Wang, W. Jin, G. Shen and R. Yu, Solvatochromogenic flavone dyes for the detection of water in acetone, *Anal. Chim. Acta*, 1999, **383**, 299–307.

26 J. S. Kim, M. G. Choi, Y. Huh, M. H. Kim, S. H. Kim, S. Y. Wang and S.-K. Chang, Determination of Water Content in Aprotic Organic Solvents Using 8-Hydroxyquinoline Based Fluorescent Probe, *Bull. Korean Chem. Soc*, 2006, **27**, 2058–2060.

27 H. Mishra, V. Misra, M. S. Mehata, T. C. Pant and H. B. Tripathi, Fluorescence Studies of Salicylic Acid Doped Poly(vinyl alcohol) Film as a Water/Humidity Sensor, *J. Phys. Chem. A*, 2004, **108**, 2346–2352.

28 A. C. Kumar and A. K. Mishra, 1-Naphthol as an excited state proton transfer fluorescent probe for sensing bound-water hydration of polyvinyl alcohol, *Talanta*, 2007, **71**, 2003–2006.

29 Y. Ooyama, M. Sumomogi, T. Nagano, K. Kushimoto, K. Komaguchi, I. Imae and Y. Harima, Detection of water in organic solvents by photo-induced electron transfer method, *Org. Biomol. Chem.*, 2011, **9**, 1314–1316.

30 Y. Ooyama, A. Matsugasako, K. Oka, T. Nagano, M. Sumomogi, K. Komaguchi, I. Imae and Y. Harima, Fluorescence PET (photo-induced electron transfer) sensors for water based on anthracene–boronic acid ester, *Chem. Commun.*, 2011, **47**, 4448–4450.

31 Y. Ooyama, A. Matsugasako, Y. Hagiwara, J. Ohshita and Y. Harima, Highly sensitive fluorescence PET (photo-induced electron transfer) sensor for water based on anthracene–bisboronic acid ester, *RSC Adv.*, 2012, **2**, 7666–7668.

32 Y. Ooyama, K. Furue, K. Uenaka and J. Ohshita, Development of highly-sensitive fluorescence PET (photo-induced electron transfer) sensor for water: anthracene–boronic acid ester, *RSC Adv.*, 2014, **4**, 25330–25333.

33 Y. Ooyama, M. Hato, T. Enoki, S. Aoyama, K. Furue, N. Tsunoji and J. Ohshita, A BODIPY sensor for water based on a photo-induced electron transfer method with fluorescence enhancement and attenuation systems, *New J. Chem.*, 2016, **40**, 7278–7281.

34 Y. Ooyama, R. Sagisaka, T. Enoki, N. Tsunoji and J. Ohshita, Tetraphenylethene– and diphenyldibenzofulvene–anthracene-based fluorescence sensors possessing photo-induced electron transfer and aggregation-induced emission enhancement characteristics for detection of water, *New J. Chem.*, 2018, **42**, 13339–13350.

35 D. Jinbo, K. Imato and Y. Ooyama, Fluorescent sensor for water based on photo-induced electron transfer and Förster resonance energy transfer: anthracene-(aminomethyl)phenylboronic acid ester-BODIPY structure, *RSC Adv.*, 2019, **9**, 15335–15340.

36 D. Jinbo, K. Ohira, K. Imato and Y. Ooyama, Development of fluorescent sensors based on a combination of PET (photo-induced electron transfer) and FRET (Förster resonance energy transfer) for detection of water, *Mater. Adv.*, 2020, **1**, 354–362.

37 L. Ding, Z. Zhang, X. Li and J. Su, Highly sensitive determination of low-level water content in organic solvents using novel solvatochromic dyes based on thioxanthone, *Chem. Commun.*, 2013, **49**, 7319–7321.

38 Y. Zhang, D. Li, Y. Li and J. Yu, Solvatochromic AIE luminogens as supersensitive water detectors in organic solvents and highly efficient cyanide chemosensors in water, *Chem. Sci*, 2014, **5**, 2710–2716.

39 Y. Mise, K. Imato, T. Ogi, N. Tsunoji and Y. Ooyama, Fluorescence sensors for detection of water based on tetraphenylethene–anthracene possessing both solvatofluorochromic properties and aggregation-induced emission (AIE) characteristics, *New J. Chem.*, 2021, **45**, 4164–4173.

40 N. Zhao, Z. Yang, J. W. Y. Lam, H. H. Y. Sung, N. Xie, S. Chen, H. Su, M. Gao, I. D. Williams, K. S. Wong and B. Z. Tang, Benzothiazolium-functionalized tetraphenylethene: an AIE luminogen with tunable solid-state emission, *Chem. Commun.*, 2012, **48**, 8637–8639.

41 X. Y. Shen, Y. J. Wang, H. Zhang, A. Qin, J. Z. Sun and B. Z. Tang, Conjugates of tetraphenylethene and diketopyrrolopyrrole: tuning the emission properties with phenyl bridges, *Chem. Commun.*, 2014, **50**, 8747–8750.

42 F. Khan, A. Ekbote, S. M. Mobin and R. Misra, Mechanochromism and Aggregation-Induced Emission in Phenanthroimidazole Derivatives: Role of Positional Change of Different Donors in a Multichromophoric Assembly, *J. Org. Chem.*, 2021, **86**, 1560–1574.

43 Q. Deng, Y. Li, J. Wu, Y. Liu, G. Fang, S. Wang and Y. Zhang, Highly sensitive fluorescent sensing for water based on poly(*m*-aminobenzoic acid), *Chem. Commun.*, 2012, **48**, 3009–3011.

44 W.-E. Lee, Y.-J. Jin, L.-S. Park and G. Kwak, Fluorescent Actuator Based on Microporous Conjugated Polymer with Intramolecular Stack Structure, *Adv. Mater.*, 2012, **24**, 5604–5609.

45 D.-C. Han, Y.-J. Jin, J.-H. Lee, S.-I. Kim, H.-J. Kim, K.-H. Song and G. Kwak, Environment-Specific Fluorescence Response of Microporous, Conformation-Variable Conjugated Polymer Film to Water in Organic Solvents: On-line Real-Time Monitoring in Fluidic Channels, *Macromol. Chem. Phys.*, 2014, **215**, 1068–1076.

46 J. Lee, M. Pyo, S. Lee, J. Kim, M. Ra, W.-Y. Kim, B. J. Park, C. W. Lee and J.-M. Kim, Hydrochromic conjugated polymers for human sweat pore mapping, *Nat. Commun.*, 2014, **5**, 3736.

47 T. Fumoto, S. Miho, Y. Mise, K. Imato and Y. Ooyama, Polymer films doped with fluorescent sensor for moisture and water droplet based on photo-induced electron transfer, *RSC Adv.*, 2021, **11**, 17046–17050.

48 W. Yang, H. Fan, X. Gao, S. Gao, V. Vardhan, R. Karnati, W. Ni, W. B. Hooks, J. Carson, B. Weston and B. Wang, The First Fluorescent Diboronic Acid Sensor Specific for Hepatocellular Carcinoma Cells Expressing Sialyl Lewis X, *Chem. Biol.*, 2004, **11**, 439–448.

49 Y.-I. Lin, S. A. Lang Jr., C. M. Seifert, R. G. Child, G. O. Morton and P. F. Fabio, Aldehyde Syntheses. Study of the preparation of 9,10-anthracenedicarboxaldehyde, *J. Org. Chem.*, 1979, **44**, 4701–4703.